Supplemental figures and legends

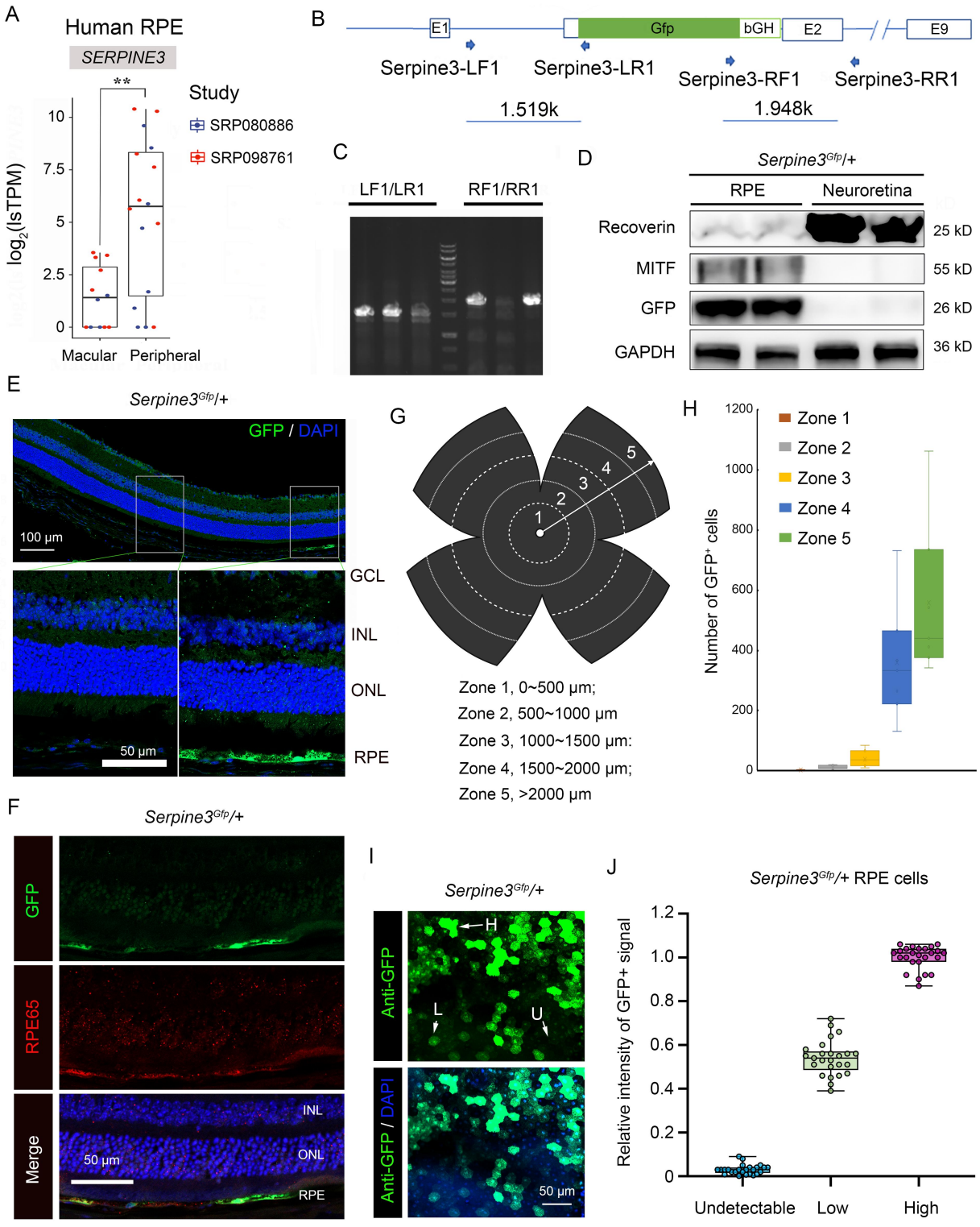

Supplemental Figure 1. Serpine3-GFP^{+}-RPE cells are concentrated at the peripheral area in *Serpine3^{Gfp}*/+ mice at postnatal 2 months. (A) Dot plots of SERPINE3 expression in the human macular and peripheral RPE from the RNA-seq

data (SRP080886 and SRP098761). (B) Schematic diagram of primer design for genotyping. (C) PCR images amplifying the Serpine3-Gfp sequences from gene-edited mice. (D) Western blotting shows GFP expression in RPE and neuroretina (n=4). (E) Images of anti-GFP immunostaining in *Serpine3*^{Gfp}/+ mice at 2 months; GFP signal appears only in the RPE of *Serpine3*^{Gfp}/+ mice. (F) Sectional immunostaining of anti-GFP and anti-RPE65 in retina (n=4). (G) Schematic diagram of flat-mount RPE shows 5 analyzed zones. (H) Quantification of GFP+ cells localized at these zones (n=7). (I, J) RPE flat mount immunostaining of anti-GFP in in *Serpine3*^{Gfp}/+ mice at 2 months and quantification of GFP^{+} signal intensity in the peripheral RPE with varying levels (n=5). GCL, ganglion cell line; INL, inner nuclear layer; ONL, outer nuclear layer; RPE, retinal pigment epithelium. Data presented as mean ± SD (G). DESeq2 was used to determine the different expression of *SERPINE3* (B). **<0.01.

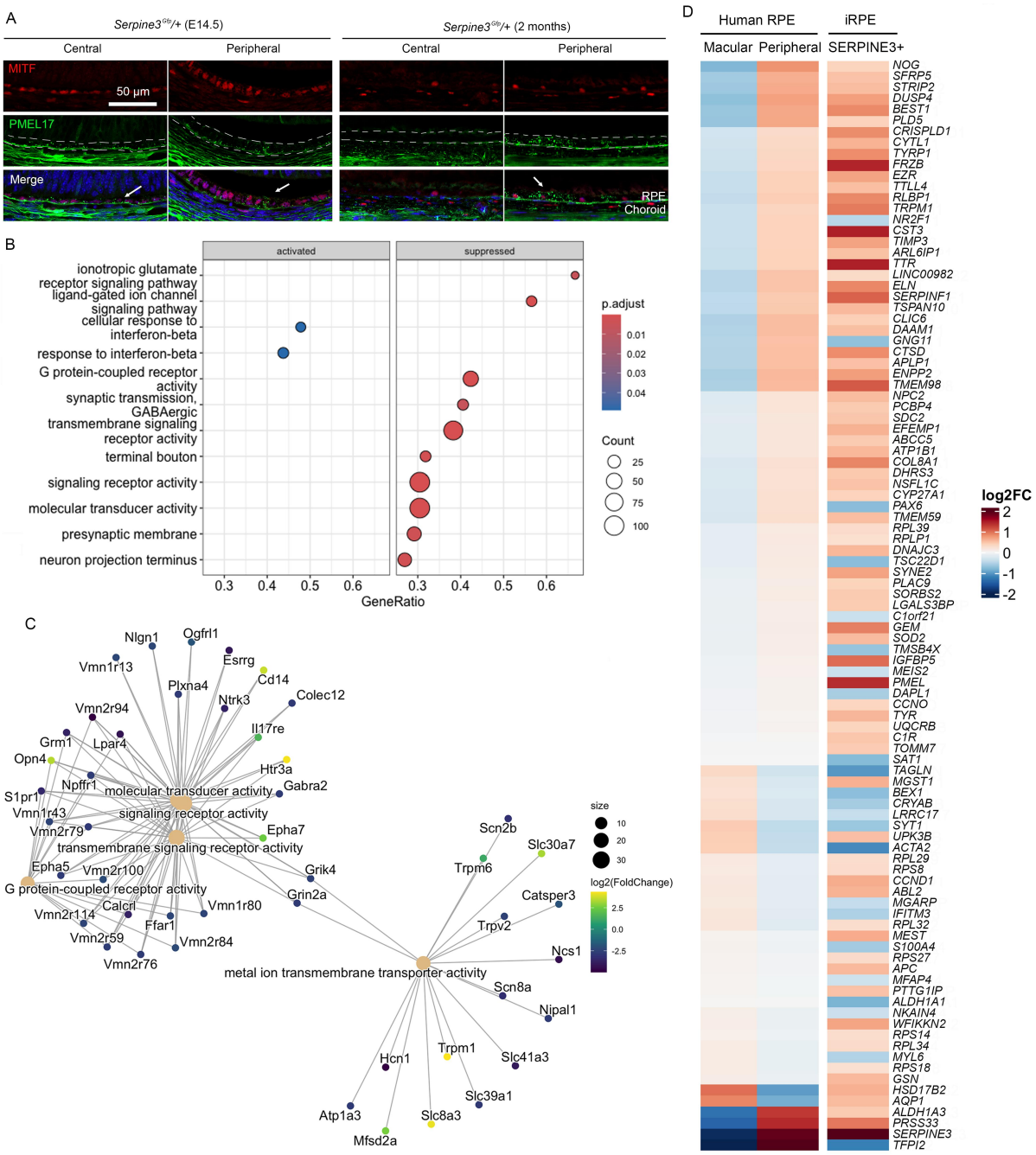

Supplemental Figure 2. Transcriptomic analysis of GFP+ RPE cells from 2-month-old *Serpine3*^{Gfp}/+ mice and SERPINE3^{+} RPE cells derived from human iPSCs. (A) Immunostaining for anti-PEML17 and anti-MITF in *Serpine3*^{Gfp}/+ mouse retinal sections at embryonic day 14.5 (left) and 2 months (right), showing marker localization in RPE cells. (B) Dot plots from Gene Set Enrichment Analysis (GSEA) presenting the top 12 signaling pathways with differential activation or inactivation in GFP^{+} RPE cells. (C) CNet plots visualize differentially expressed genes (DEGs),

grouped by pathway and colored by up- or downregulation relative to central GFP^{-}RPE control cells. (D) A heat map compares the gene expression profiles of SERPINE3^{+}-iRPE cells with those of human macular and peripheral RPE cells, highlighting similarities and differences.

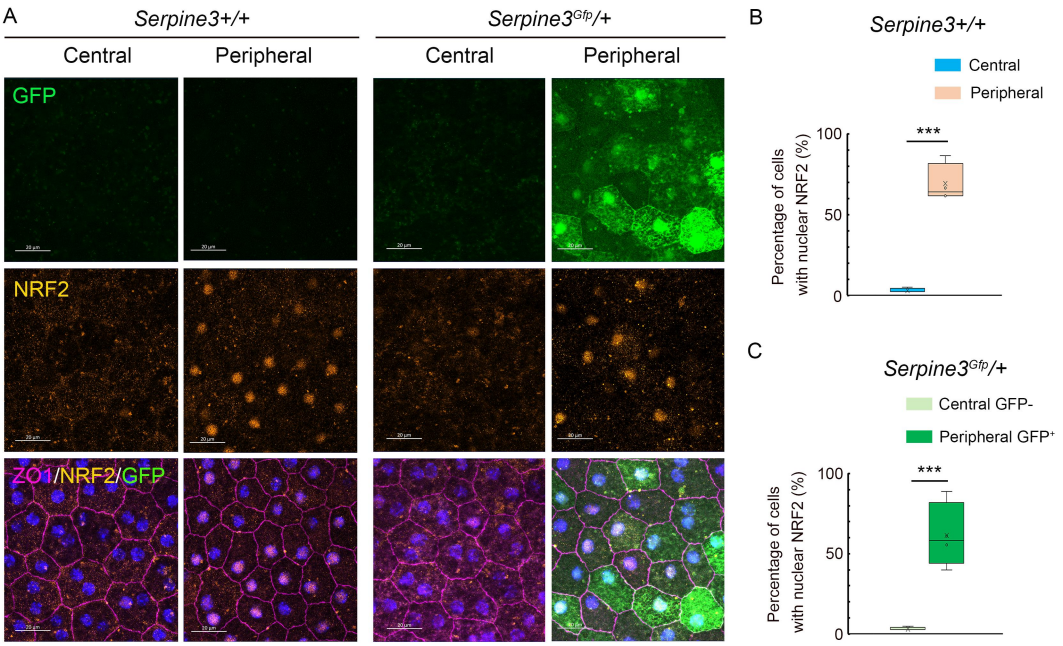

Supplemental Figure 3. Nuclear localization of NRF2 is enriched in peripheral GFP$^+$ cells from 2-month-old *Serpine3^{Gfp}*/+ mice. (A) RPE flat-mount immunostaining of anti-GFP, anti-NRF2 and anti-ZO1 in the *Serpine3*+/+ and *Serpine3^{Gfp}*/+ mice (n=4). (B, C) Quantification of the percentage of cells with nuclear NRF2 in the peripheral and central RPE cells from *Serpine3*+/+ (B) and *Serpine3^{Gfp}*/+ mice (C). Data indicate the mean ± SD (B, C). Statistics were calculated by unpaired 2-tailed Student's *t* test (B, C). ***P<0.001.

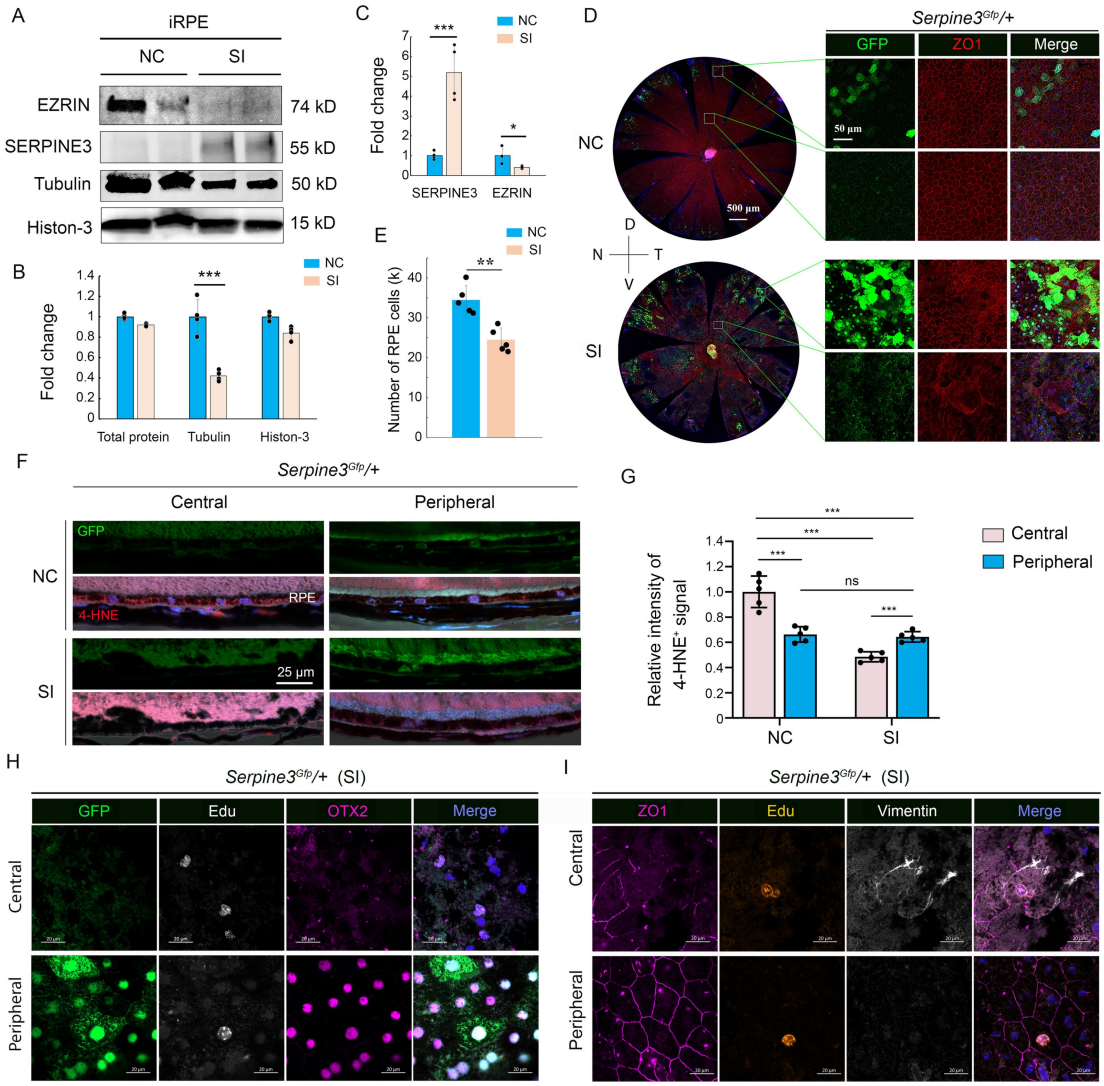

Supplemental Figure 4. GFP⁺-RPE cells can survive and regenerate new RPE cells in *Serpine3*^{Gfp}/+ mice after sodium iodate treatment. (A-C) Western blotting and dot quantification show a significant increase in SERPINE3 and a sharp decrease in EZRIN in iRPE cells after SI treatment (n=4). (D) Immunostaining images of anti-GFP and anti-ZO1 in RPE from 2-month-old *Serpine3*^{Gfp}/+ mice with saline (upper panels) or sodium iodate (lower panels) treatment. (E) Bar graphs show a decrease in GFP+ RPE cells in *Serpine3*^{Gfp}/+ mice after SI injury (n=4). (F, G) Retinal sectional immunostaining of anti-4-HNE and anti-GFP in the *Serpine3*^{Gfp}/+ mice (F) and the quantification of 4-HNE signal intensity in the peripheral and central RPE under physiologic or SI-injured conditions (G) (n=5). (H, I) Immunostaining images of anti-GFP and anti-OTX2 (H) or anti-Vimentin (I) with Edu staining in flat-mount RPE of *Serpine3*^{Gfp}/+ mice after SI treatment (n=4). Data presented as

mean ± SD. Statistics were calculated by unpaired 2-tailed Student's *t* test (B, C and E), or 2-way ANOVA followed by Tukey's test (G). **P<0.01, ***P<0.001.

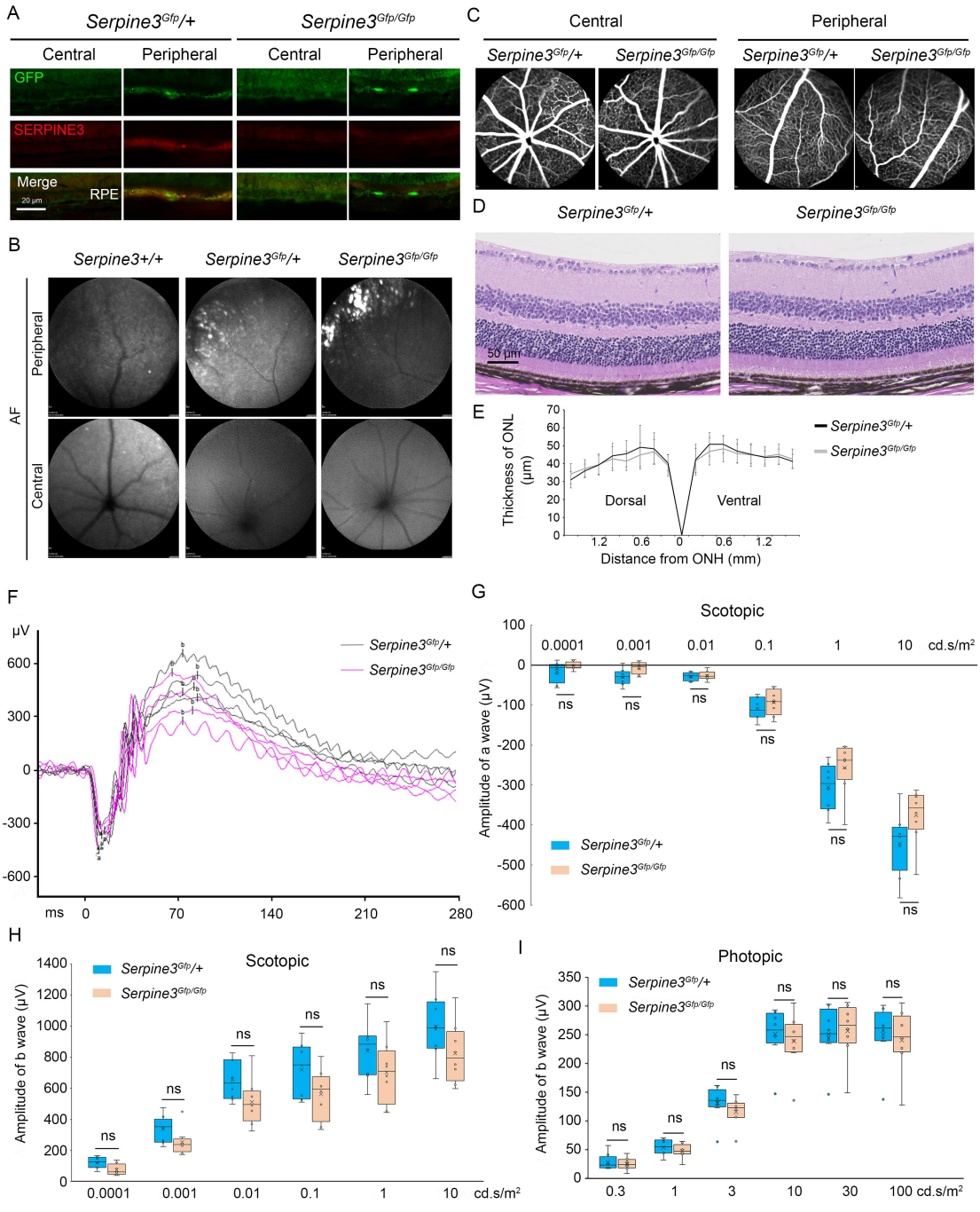

Supplemental Figure 5. Deletion of SERPINE3 does not affect the survival of GFP+-RPE cells, retinal delamination, pigmentation, or retinal function in young mice. (A) Retinal sectional immunostaining of anti-GFP and anti-SERPINE3 in the *Serpine3*^{Gfp}/+ and *Serpine3*$^{Gfp/Gfp}$ mice. (B) Autofluorescence fundus images show peripheral and central retinas from *Serpine3*+/+, *Serpine3*^{Gfp}/+, or *Serpine3*$^{Gfp/Gfp}$ mice at 2 months. (C) Autofluorescence fundus images of *Serpine3*^{Gfp}/+ and *Serpine3*$^{Gfp/Gfp}$ mice after 5 minutes of fluorescence sodium

injection. (D and E) Histological images of the retinas (D) and quantification of outer nuclear layer thickness (E) from *Serpine3*$^{Gfp/+}$ and *Serpine3*$^{Gfp/Gfp}$ mice at 2 months. (F) Scotopic ERG traces of *Serpine3Gfp/+* and *Serpine3*$^{Gfp/Gfp}$ mice at 2 months with flashlight stimulation (10(S)cd.s/m2). (G-I) Quantification of the amplitude of scotopic a wave (G), scotopic b wave (H) and photopic b wave (I) in *Serpine3*^{Gfp}*/+* and *Serpine3*$^{Gfp/Gfp}$ mice at 2 months under the indicated condition. Data presented as mean ± SD. Statistics were calculated by unpaired 2-tailed Student's *t* test (E, G and H).

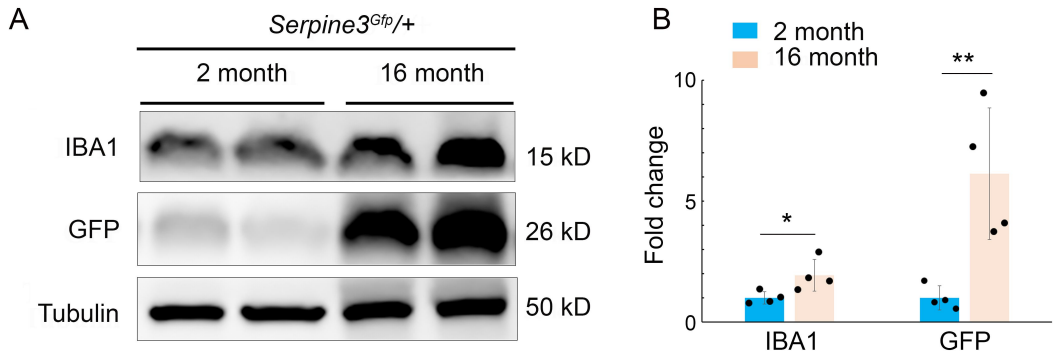

Supplemental Figure 6. GFP levels increase in aged *Serpine3*^{Gfp}/+ mice. (A) Western blotting images showing EZRIN, IBA1 and GFP proteins in the RPE tissue from *Serpine3*^{Gfp}/+ mice at 2 and 16-months old. (B) Quantification of dot bolts of IBA1 and GFP signals in the RPE from the *Serpine3*^{Gfp}/+ mice at 2 and 16-months old (n=4). Data presented as mean ± SD. Statistics were calculated by unpaired 2-tailed Student's *t* test (B). *P<0.05, **P<0.01.

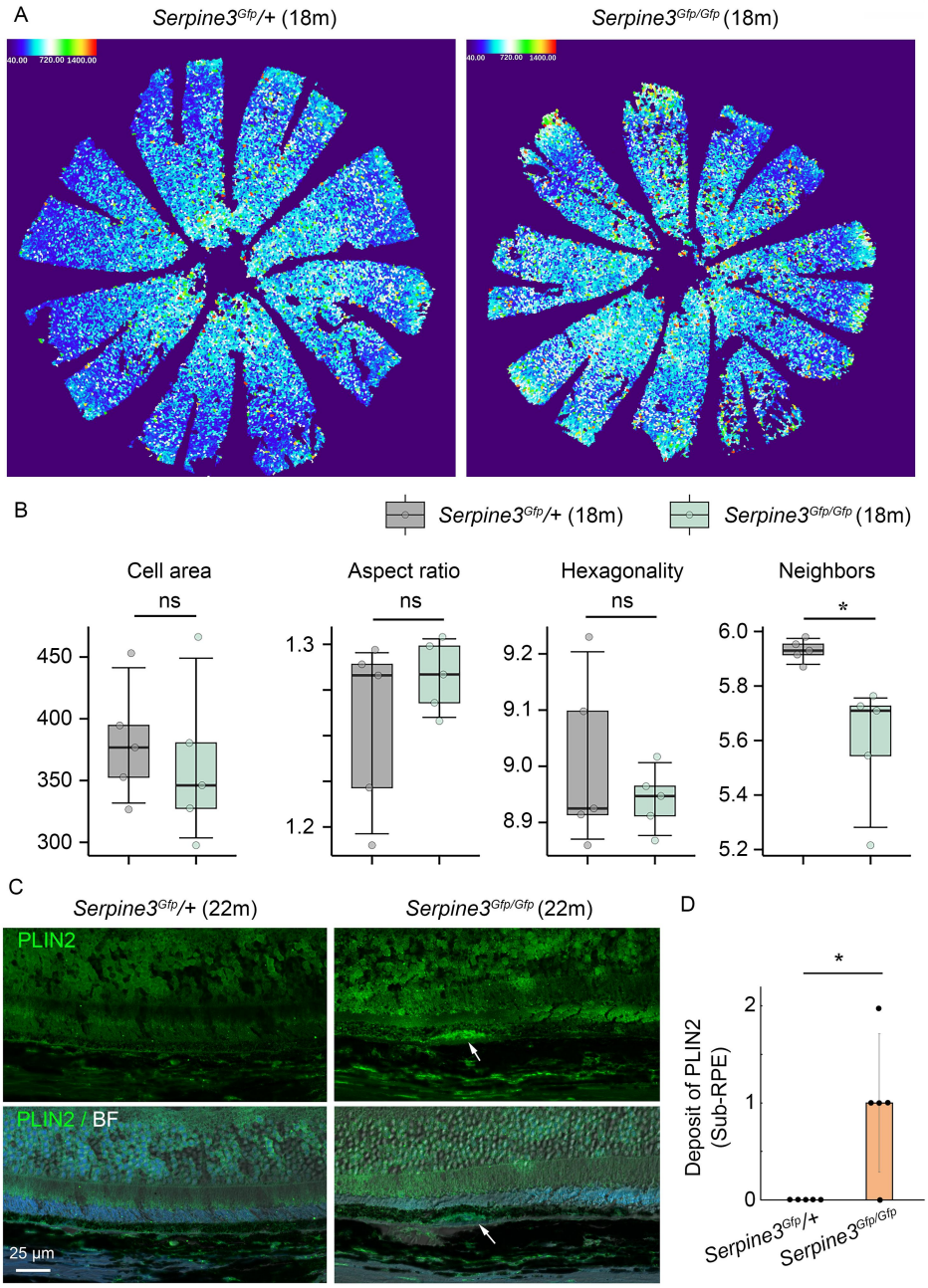

Supplemental Figure 7. Reshape analysis of the aged *Serpine3*^{Gfp}/+ and *Serpine3*$^{Gfp/Gfp}$ RPE. (A) The reshaped images of RPE flat-mount immunostaining of anti-ZO1 in the *Serpine3*^{Gfp}/+ and *Serpine3*$^{Gfp/Gfp}$ mice at 18 months old. (B) The statistical analysis of the RPE cells from the aged *Serpine3*^{Gfp}/+ and *Serpine3*$^{Gfp/Gfp}$ mice for the cell area, aspect ratio, hexagonality and neighbors in the dorsal area. (C and D) Immunostaining for anti-PLIN2 on retinal section from 22-month-old *Serpine3*^{Gfp}/+ and *Serpine3*$^{Gfp/Gfp}$ mice (C) and the quantification of PLIN2 deposits

at the sub-RPE space (D). Data presented as mean ± SD. Statistics were calculated by unpaired 2-tailed Student's *t* test (B, D). *P<0.05.

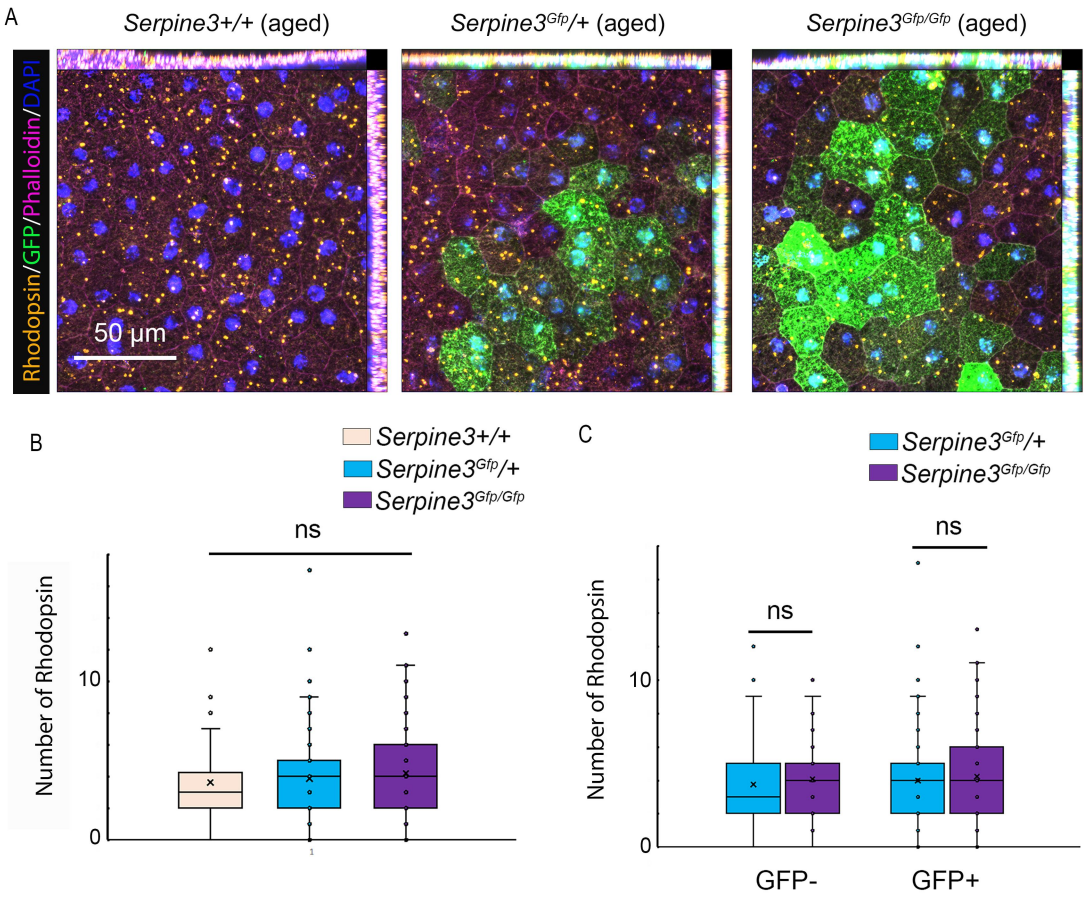

Supplemental Figure 8. Deficiency of SERPINE3 does not affect RPE phagocytosis. (A) RPE flat-mount immunostaining images of anti-GFP and anti-Rhodopsin combined with phalloidin staining in 16-month-old wildtype, *Serpine3*^{Gfp}/+ and *Serpine3*$^{Gfp/Gfp}$ mice (n=5). (B) Quantification of the number of Rhodopsin^{+} particles in each single RPE cell from the aged wildtype, *Serpine3*^{Gfp}/+ and *Serpine3*$^{Gfp/Gfp}$ mice (n=5). (C) Quantification of the number of Rhodopsin^{+} particles in each single GFP^{+} or GFP^{-} RPE cells from the aged *Serpine3*^{Gfp}/+ and *Serpine3*$^{Gfp/Gfp}$ mice (n=5). Data presented as mean ± SD. Statistics were calculated by 2-way ANOVA followed by Tukey's test (B).

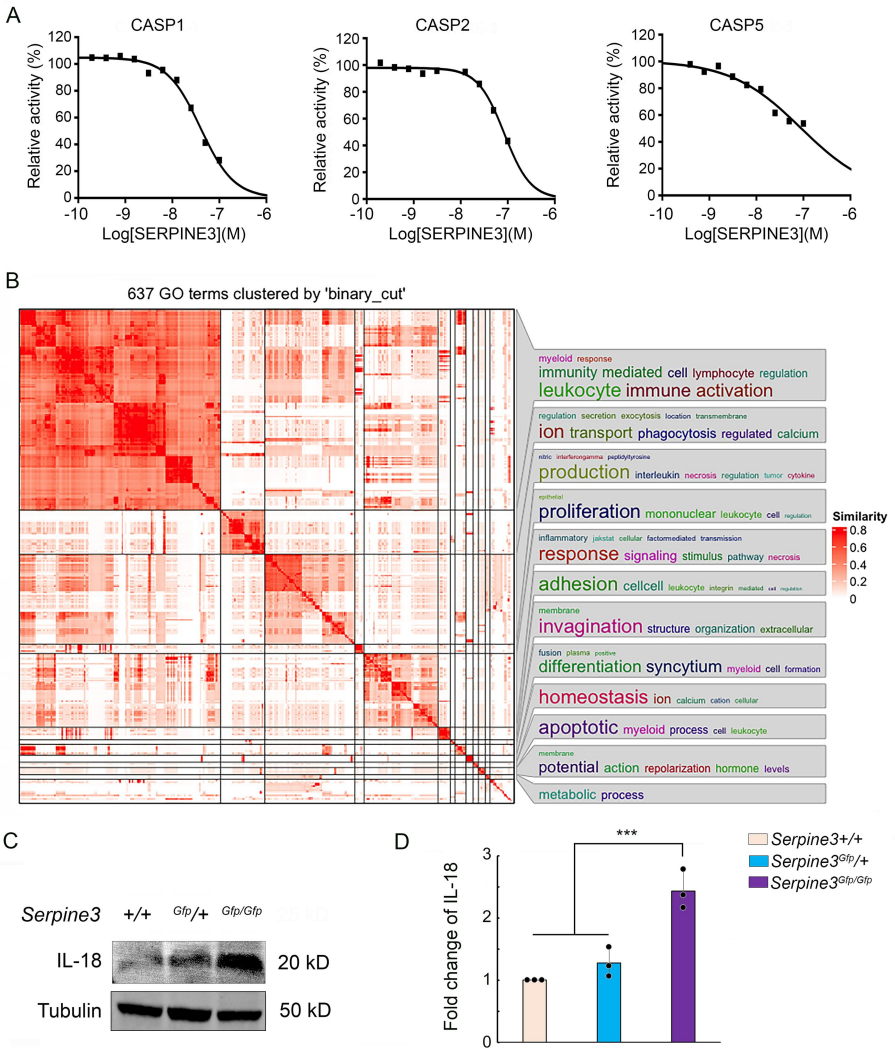

Supplemental Figure 9. SERPINE3 binds Caspase-1 and inhibits Caspase-1 activity. (A) Curve graphs show the activity of CASPASE1, CASPASE2 and CASPASE5 under the treatment of SERPINE3 at different dosages. (B) Heatmap shows the GO analysis of bulk RNA-seq from the RPE/choroidal tissue of 18-month-old *Serpine3*^{Gfp}/+ and *Serpine3*$^{Gfp/Gfp}$ mice. (C and D) Western blotting (C) and quantification of the dots (D) show a significant increase in IL-18 in aged *Serpine3*$^{Gfp/Gfp}$ mice (n=3). ***<0.001. Data presented as mean ± SD. Statistics were calculated by 2-way ANOVA followed by Tukey's test (D).

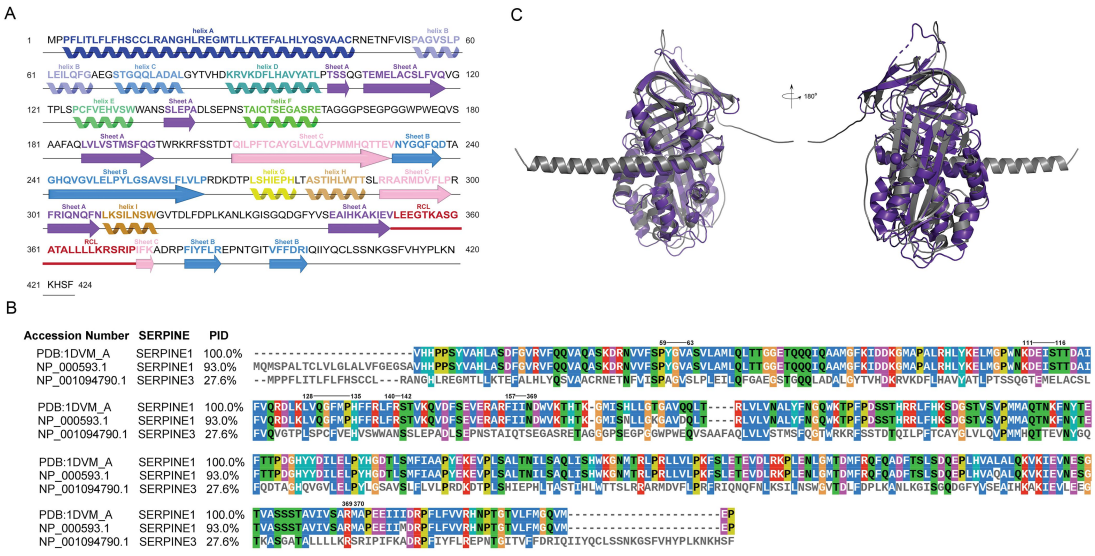

Supplemental Figure 10. Alignment analysis between SERPINE1 and SERPINE3. (A) Multiple sequence alignment among SERPINE1 and SERPINE3 sequences. PID indicates percentage identity. (B) Structure alignment between the SERPINE3 predicted protein structure (gray) and the SERPINE1 protein structure (purple).

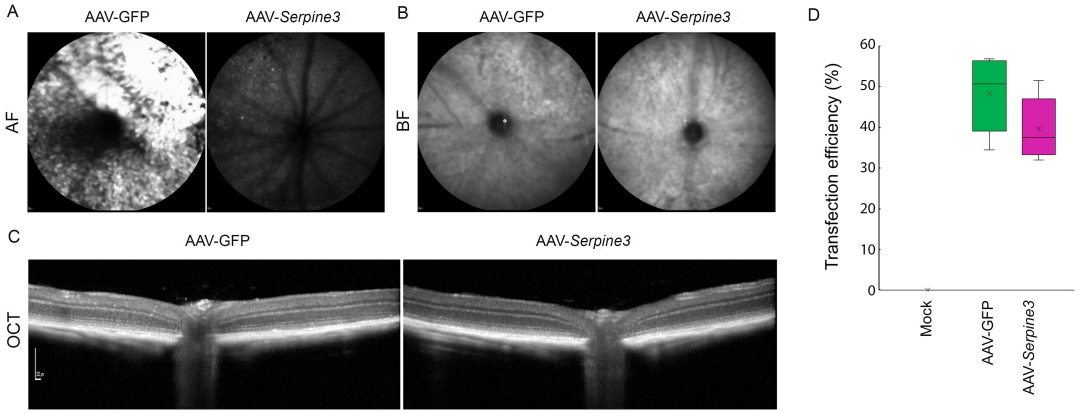

Supplemental Figure 11. AAV-Serpine3 transduction does not cause any detectable changes in 2-month-old C57BL/6J mice. (A, B) Four weeks after AAV transduction, autofluorescence (A) and bright field (B) fundus images are shown. (C) OCT images of retinal structures in mice transduced with AAV-GFP or AAV-SERPINE3 for 4 weeks. (D) Bar graphs show transduction efficiency for both vectors at 4 weeks post-injection.

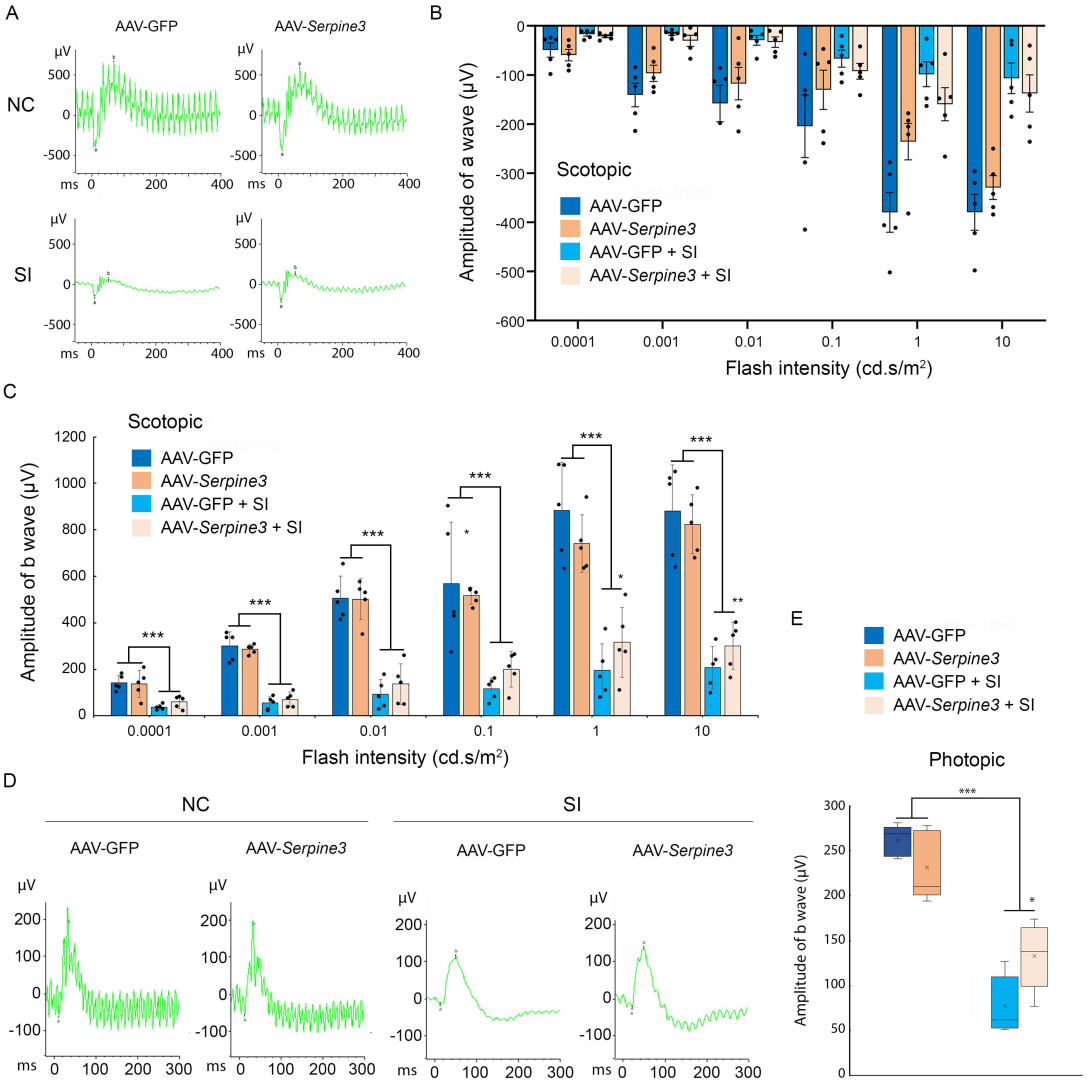

Supplemental Figure 12. AAV-SERPINE3 confers marginal preservation of retinal function in the SI injury model. (A) Scotopic ERG traces at 10 cd·s/m² from wildtype mice transduced with AAV-GFP or AAV-Serpine3, with or without SI treatment. (B, C) Quantification of a-wave (B) or b-wave (C) amplitude at flash intensities from 0.0001 to 10 cd·s/m². (D, E) Photopic ERG traces (D) and b-wave amplitude quantification (E) at 30 cd·s/m² (n=5). Data presented as mean ± SD. Statistics were calculated by paired 2-tailed Student's t test (B, C and E). *<0.05, **<0.01, ***<0.001.